Available online at www.sciencedirect.com
SCIENCE DIRECT
Biochemical and Biophysical Research Communications 345 (2006) 229–238
BBRC
www.elsevier.com/locate/ybbrc

Testicular proteins associated with the germ cell-marker, TEX101: Involvement of cellubrevin in TEX101-trafficking to the cell surface during spermatogenesis

Hiroki Tsukamoto [a], Hiroshi Yoshitake [a], Miki Mori [b], Mitsuaki Yanagida [a], Kenji Takamori [a], Hideoki Ogawa [a], Toshihiro Takizawa [b], Yoshihiko Araki [a,*]

[a] *Institute for Environmental and Gender-Specific Medicine, Juntendo University Graduate School of Medicine, Urayasu-City 279-0021, Japan*
[b] *Department of Molecular Anatomy, Nippon Medical School, Tokyo 113-8602, Japan*

Received 6 April 2006
Available online 25 April 2006

Abstract

Recently, we identified a cell-surface marker protein, TEX101, that is unique to male and female germ cells. On/off switching of TEX101 expression in germ cells is closely linked to the kinetics of gametogenesis. In the present study, we isolated testicular proteins by immunoprecipitation with anti-TEX101 antibody and identified the proteins using liquid chromatography/tandem mass spectrometry. Of three proteins identified (annexin 2, ly6k, and cellubrevin), a biochemical association between TEX101 and cellubrevin was confirmed by immunoprecipitation-Western blotting experiments. Immunohistochemistry using a cellubrevin-specific antibody indicated that the molecule is abundant on spermatocytes and early-stage spermatids, whereas negligible amounts are found in Sertoli cells, spermatogonia, spermatozoa, and late-stage spermatids. Most of the intracellular cellubrevin appeared to be juxtaposed with intracellular TEX101, and membrane-associated cellubrevin was docked near TEX101-positive plasma membranes on the cytoplasmic side. This close association was never observed on the outer surface of the plasma membrane. From these results we concluded that cellubrevin-dependent membrane trafficking is involved in TEX101-transport to the surface of male germ cells.

Keywords: TEX101; Cellubrevin; Germ cell; Testis; Mouse; Spermatogenesis; Proteomics; Glycosylphosphatidylinositol-anchored protein

It is well known that the gonadal organs play physiological roles crucially on the production of gametes, i.e., eggs and spermatozoa. In mammalian testis, spermatogenesis occurs within the seminiferous tubules after the onset of the puberty [1–3]. Spermatogonia proliferate around the basement membrane and produce daughter cells known as spermatocytes and spermatids, which undergo two consecutive meiotic divisions. These meiotic cells migrate progressively across the seminiferous epithelium while maintaining contact with nourishing Sertoli cells. Finally, the resulting round spermatids detach from the seminiferous epithelium during spermiogenesis and are transported to the epididymis as viable spermatozoa. Although the morphology of spermatogenesis has been well characterized, its underlying molecular mechanisms and genetic regulation are far from completely understood.

In addition to regulation by components of the endocrine system including gonadotrophins and other sexual hormones, spermatogenesis is also regulated by testicular intercellular mechanisms such as secretion of humoral factors and direct cell–cell interaction [4–6]. Indeed, the morphology of the testis is exquisitely designed to promote survival and maturation of germ cells to become gametes [4,5]. The spatially and temporally ordered arrangement of differentiating germ cells within the seminiferous tubules suggests that gene expression in, and differentiation of, germ cells is precisely coordinated [7,8]. To date, the list of genes and proteins that are known to be expressed in germ cells is rapidly growing

* Corresponding author. Fax: +81 47 353 3178.
E-mail address: yaraki@med.juntendo.ac.jp (Y. Araki).

0006-291X/$ - see front matter © 2006 Elsevier Inc. All rights reserved.
doi:10.1016/j.bbrc.2006.04.070

[9–11], and some of the molecules exhibiting stage-specific expression are believed to play essential roles in spermatogenesis [12–18]. Although the tyrosine kinase-type c-kit receptor [19] has been reported as a key spermatogenetic factor, there have been relatively few other plasma membrane proteins that have been identified as such. Since gene expression can affect many of the functions of germ cells, including signal transduction, the uptake of bioactive molecules, cell adhesion, and cell migration, gene expression in germ cells is generally thought to be tightly regulated in that the cells are responsive to the extracellular milieu which varies with the stage of the seminiferous epithelium. Therefore, if we can unravel the relationship between the spatiotemporal expression kinetics of germ cell surface molecules and their molecular functions, our understanding of spermatogenesis will be greatly enhanced.

We previously raised a mouse IgG1 monoclonal antibody (mAb) against stage/cell-specific testicular antigen. This mAb, designated TES101, was used to identify a novel, germ-cell-specific protein, TEX101 (TES101-reactive protein)[20], which is a cell-surface marker unique to male and female germ cells [20–22]. In the fetal testis, TEX101 first appears on the plasma membrane of prospermatogonia within immature seminiferous cords [21]. After puberty, it no longer appears on the spermatogonia; it appears, instead, on meiotic cells including spermatocytes, spermatids, and testicular sperm [21]. Finally, it is shed from the cell surface of epididymal sperm during transport through the caput epididymis duct [22]. In contrast, TEX101 is transiently expressed in oogonia and oocytes until the start of folliculogenesis in the developing ovary [21]. The sexual dimorphism of TEX101 expression kinetics suggests that TEX101 plays an important physiological role during germ cell development and differentiation.

Molecular biological and biochemical analyses of TEX101 have shown that it is a 250-amino acid polypeptide with strongly hydrophobic signal peptides at both the N- and C-termini [20], which constitutes a typical feature of glycosylphosphatidylinositol (GPI)-anchored proteins [23]. Using a transient expression system in mammalian cells, we recently confirmed that TEX101 is anchored to the cell-surface membrane via its GPI-moiety [24]. Intriguingly, the TEX101 amino acid sequence indicates no apparent homology to any molecules in the DNA/protein databases [20]. Although this unique structure is of interest in the field of structural biology, it also prevents us from forming homology-based hypotheses about its physiological role. In this situation, a reasonable alternative approach is to identify the molecules that associate with TEX101, since many proteins physically associate with some of the other proteins that influence their biological activities (e.g., by providing substrates or by regulating activity) [25].

In the present study, we identified proteins in mouse testicular homogenate that associate with TEX101, using immunoprecipitation and liquid chromatography (LC)-tandem mass spectrometry (MS/MS). Furthermore, the biochemical and morphological characteristics of the physiological associations between the identified proteins were evaluated.

Materials and methods

Animals and reagents. Male BALB/c mice (6–8-week-old) were purchased from Charles River Japan (Yokohama, Japan) and given free access to food and water. They were maintained and bred at the Animal facility, Juntendo University, under 12L:12D conditions. All animal experiments were conducted according to the guide for care and use of laboratory animals, Juntendo University.

Tissue-Tek O.C.T. compound was obtained from Sakura Finetechnical (Tokyo, Japan). EDTA-free complete inhibitor cocktail was from Roche Diagnostics GmbH (Penzberg, Germany). Protein G–Sepharose 4 FF was purchased from Amersham Biosciences (Piscataway, NJ, USA). Zenon™ Alexa Fluor® 488 mouse IgG1 labeling kits and ProLong® Antifade kit were from Invitrogen (Carlsbad, CA, USA). Sequencing grade-modified trypsin was obtained from Promega (Madison, WI, USA), and 4′,6-diamidino-2-phenylindole dihydrochloride (DAPI) was from Molecular Probes (Eugene, OR, USA), respectively. The glass slides and coverslips for microscopic observation were purchased from Matsunami Glass (Osaka, Japan). All other chemicals were commercially obtained and were of the highest purity available.

Antibodies. Mouse anti-TEX101 mAb (TES101, IgG1) was prepared as described previously [20]. Mouse anti-human GPI-80 mAb (3H9, IgG1) [26] was used as an isotype control for TES101 mAb in some experiments. Rabbit anti-cellubrevin polyclonal Ab was purchased from Abcam (Cambridge, UK). Mouse anti-annexin 2 mAb was obtained from BD Biosciences (San Jose, CA, USA). Highly cross-adsorbed Alexa Fluor® 594-conjugated goat anti-rabbit IgG Ab was from Invitrogen. Alexa Fluor® 488-labeled goat anti-rabbit IgG Ab was purchased from Molecular Probes. Normal rabbit Ig, horseradish peroxidase (HRP)-conjugated rabbit anti-mouse Ig Ab, and HRP-conjugated goat anti-rabbit Ig Ab were obtained from DakoCytomation (Glostrup, Denmark).

Preparation of mouse testicular extract and immunoprecipitation. Mouse testicular Triton® X-100-soluble fraction was prepared as previously described [20] with slight modification. Briefly, a testis from sexually mature mouse (approximately 50–100 mg) was homogenized with a glass homogenizer 20 strokes in nine volumes of the extraction buffer (10 mM Tris (pH 7.5), 150 mM sodium chloride, and 1× EDTA-free complete inhibitor cocktail). All the subsequent steps were performed at 4 °C or on ice. After the centrifugation at 18,000*g* for 15 min, the precipitate was resuspended in nine volumes of the extraction buffer containing 1% Triton® X-100 and then extracted by Polytron® PT3100 homogenizer (Kinematica AG, Littau-Lucerme, Switzerland) for 10 s. Following a 20-min incubation, the suspension was centrifuged for 15 min at 18,000*g*, and resultant supernatant was used as a Triton® X-100-soluble fraction, a starting material for immunoprecipitation.

Prior to the immunoprecipitation, 500 μl of the solution was precleared with 50 μl of 50% slurry of protein G–Sepharose 4 FF on a rotary shaker for 3 h. After the centrifugation for 30 s at 18,000*g*, the supernatant was incubated with primary Ab (5–60 μg), rotating overnight, and 50% slurry of protein G–Sepharose 4 FF (50 μl) was then added into the identical tubes. After an additional 3-h rotation, bound beads were separated by the centrifugation at 18,000*g* for 30 s and then washed three times with 1 ml of the extraction buffer containing 1% Triton® X-100. Precipitated beads were boiled for 3 min in a buffer for SDS–PAGE described by Laemmli [27] under reducing or non-reducing conditions. After the centrifugation, the supernatants were used as samples for SDS–PAGE.

SDS–PAGE and silver staining. The protein solutions were separated by SDS–PAGE system of Laemmli [27] using 30% acrylamide-0.8% piperazine diacrylamide solution. Following silver staining was performed using PlusOne Silver Staining kit (Amersham Biosciences), according to the manufacturer's instructions with slight modification for mass spectrometric analysis. Briefly, the gel slab was fixed in 50% ethanol/20% acetic acid for 30 min at room temperature. After the rinsing with water 5 min,

the gel was sensitized by a 30-min incubation in 30% ethanol containing 0.2% sodium thiosulfate/6.8% sodium acetate. Following the sensitization, the gel was rinsed three times with distilled water for 5 min each and then submerged in 0.25% silver nitrate solution for 20 min. After two changes of distilled water for 1 min each, the gel slab was developed in 2.5% sodium carbonate buffer containing 0.04% formalin. When the desired intensity of staining was achieved, the reaction was terminated by washing with 1.46% EDTA disodium dihydrate. The silver-stained gels were stored in 10% acetic acid solution at 4 °C until analyzed.

In-gel trypsin digestion. In-gel trypsin digestion of the protein was performed according to the method described by Shevchenko et al. [28]. Typically, the bands of interest excised from the silver-stained gel (approximately 3 mm length fragments) were reduced with 100–200 μl of 10 mM dithioerythritol in 100 mM ammonium bicarbonate buffer at 56 °C for 1 h. Then, it was followed by the alkylation with 55 mM iodoacetamide in the same buffer at room temperature for 45 min in the dark. After the centrifugation, the supernatant was removed by aspiration and then the protein in-gel was digested by the overnight incubation with ~100 μl of trypsin solution (concentration: 12.5 ng/μl) in 50 mM ammonium bicarbonate buffer at 37 °C. Resulting peptide mixtures were extracted with 20 mM ammonium bicarbonate buffer and additional 5% formic acid/50% acetonitrile solution for three times. Finally, they were concentrated with a speed vacuum to a final volume of 5–10 μl for further analysis by LC–MS/MS.

LC–MS/MS analysis. The LC–MS/MS system was a LCQ DECA XP ion trap mass spectrometer (Thermo Electron, San Jose, CA, USA) with a nanospray ionization interface, coupled on-line with Magic2002 HPLC system (Michrom BioResources, Auburn, CA, USA). The mobile phases consisted of solvent A (0.1% formic acid) and B (0.1% formic acid/90% acetonitrile), and the chromatography was performed on a following gradient elution program at a flow rate of 70 μl/min: 5% B for 10 min, 5–45% B for 40 min, 45–95% B for 5 min, 95 % B for 5 min, and 5% B for 40 min. The flow was split with a Magic precolumn capillary splitter assembly (Michrom BioResources) and approximately 1.4 μl/min directed to a 0.2ID × 50-mm Mightysil RPC18 column (3-μm particle diameter) (Kanto Chemical Co. Inc., Tokyo, Japan). All of mass spectrometric data were collected using a triple play experiment in a positive ion mode. After the acquisition of a full MS scan (m/z: 400–2000) in the first scan, the most intense ion was isolated for the determination of charge state using a high resolution zoom scan in the second event. In the third event, a precursor ion was fragmented by collision-induced dissociation and then MS/MS spectra were automatically acquired dependent on the mass and charge state of the precursor ion selected. Resulting data were subjected to non-redundant National Center for Biotechnology Information database using Mascot search algorithm.

Western blot analysis. The protein components resolved by SDS–PAGE were electrophoretically blotted onto a polyvinylidene difluoride (PVDF) membrane (Immobilon-P™, Millipore, Bedford, MA, USA), as described previously [29,30]. The membrane was blocked in 1% skim milk/0.05% Tween 20 in PBS (pH 7.4), then the reactivity among the transferred proteins with primary Ab was assayed using HRP-conjugated secondary Ab and an ECL Western blotting detection system (Amersham Biosciences), exposed on a X-ray film (BioMax XAR Film, Eastman Kodak Company, Rochester, NY, USA) according to the manufacturer's instructions.

Confocal laser immunofluorescence microscopy. Mice testes were fixed in PBS (pH 7.4) containing 4% paraformaldehyde for 6 h at 4 °C. The samples were serially submerged with 10% sucrose in PBS for 6 h and with 20% sucrose for an additional 12 h at 4 °C. The samples embedded in Tissue-Tek O.C.T. compound were quickly frozen in a mixture of acetone and solid carbon dioxide and then stored at −80 °C until used. Cryosections (5–6 μm in thickness) were made with a cryostat CM 1900 (Leica, Nuccloch, Germany) and mounted on 3-aminopropyltriethoxysialene-coated glass microscope slides. The sections were air-dried for 30 min at room temperature and rinsed three times with PBS. After the 30-min incubation with 1% skim milk in PBS, the sections were probed with rabbit anti-cellubrevin Ab (2 μg/ml) in PBS for 45 min at room temperature and then washed three times in PBS. The sections were followed by a 30-min incubation with Alexa Fluor® 594-conjugated goat anti-rabbit IgG Ab (5 μg/ml). After rinsed with PBS three times, the sections were incubated with TES101 (5 μg/ml) labeled by Zenon™ Alexa Fluor® 488 labeling kit for 45 min at room temperature. The sections were washed three times with PBS and then mounted in ProLong® mounting medium containing Powdered ProLong® anti-fade reagent. The immunostained samples were examined with a confocal laser microscope (TCS SP2 AOBS, Leica), and the images were analyzed with Adobe Photoshop(R) 7.0 J software (Adobe Systems, San Jose, CA, USA). Control sections received the same treatment, with the exception that anti-cellubrevin Ab was replaced with normal rabbit Ig, and/or 3H9 mAb was used instead of TES101 mAb.

Ultrahigh-resolution immunofluorescence microscopy (UHR-IFM) using ultrathin cryosections. UHR-IFM was carried out as described previously [31,32]. Briefly, testes from sexually matured mice were cut into small pieces and fixed for 2 h at room temperature in 4% paraformaldehyde in 100 mM sodium cacodylate buffer (pH 7.4) containing 5% sucrose. The samples were embedded in 10% gelatin and then infiltrated with 2.3 M sucrose overnight at 4 °C. After sucrose infiltration, the samples were mounted on specimen pins designed to fit a Leica cryoultramicrotome and then frozen in liquid nitrogen. Ultrathin cryosections were cut with a Leica EM UC6 equipped with an FC6 cryounit. Sections (100-nm thickness or less) were cut, collected on droplets of 0.75% gelatin-2.0 M sucrose, followingly transferred to 3-aminopropyltriethoxysilane-coated round glass coverslips (12-mm diameter, No. 1 thickness).

The sections were incubated in 1% BSA and 5% normal goat serum in PBS for 1 h at room temperature, to block non-specific protein-binding sites. For double labeling, the testis sections were incubated with the primary Abs, TES101 (0.13–0.26 μg /ml) and rabbit anti-cellubrevin (5–10 μg/ml), for 30 min at 37 °C. The sections were subsequently incubated for 30 min at 37 °C with the secondary Abs, Alexa Fluor® 594-labeled goat anti-mouse IgG and Alexa Fluor® 488-labeled goat anti-rabbit IgG (5 μg/ml each). Finally, the tissue sections were counterstained with DAPI and then mounted in ProLong anti-photobleaching medium on glass microscope slides. Control sections received the same treatment except that the primary Ab was either omitted or replaced with purified non-immune IgG. Fluorescent images were collected with a BX60 microscope (Olympus, Tokyo, Japan) equipped with a Spot RT SE6 CCD camera (Diagnostic Instruments, Sterling Heights, MI, USA) and were captured with the MetaMorph image analysis system (Universal Imaging, Dowingtown, PA). The figures were compiled using Photoshop CS software (Adobe Systems).

Results

Identification of testicular proteins associated with TEX101

To identify testicular proteins that interact with TEX101, we initially chose a proteomic approach. Given that previous biochemical studies from our group have indicated that TEX101 is found predominantly in the Triton® X-100-soluble fraction of testicular extract obtained from sexually mature mice [20], we performed immunoprecipitation studies on this fraction using 9 μg of anti-TEX101 mAb (TES101) or 3H9 mAb (isotype-match control). To distinguish proteins originated from ascites during mAb preparation, we also carried out control experiments without the testicular fraction. After immunoprecipitation, the adsorbed proteins were separated by SDS–PAGE under reducing conditions, and the gel was visualized by silver staining. Three specific bands were clearly detected in the TES101-precipitated proteins (Fig. 1, lane 1) but not in the 3H9-precipitated proteins (Fig. 1, lane 2), or in the proteins precipitated in the absence of the testicular extract (Fig. 1, lanes 3 and 4).

Attempts were then made to identify the precipitated proteins using LC–MS/MS. As expected, a major gel band running at approximately 36 kDa (Fig. 1, 'A', lane 1)

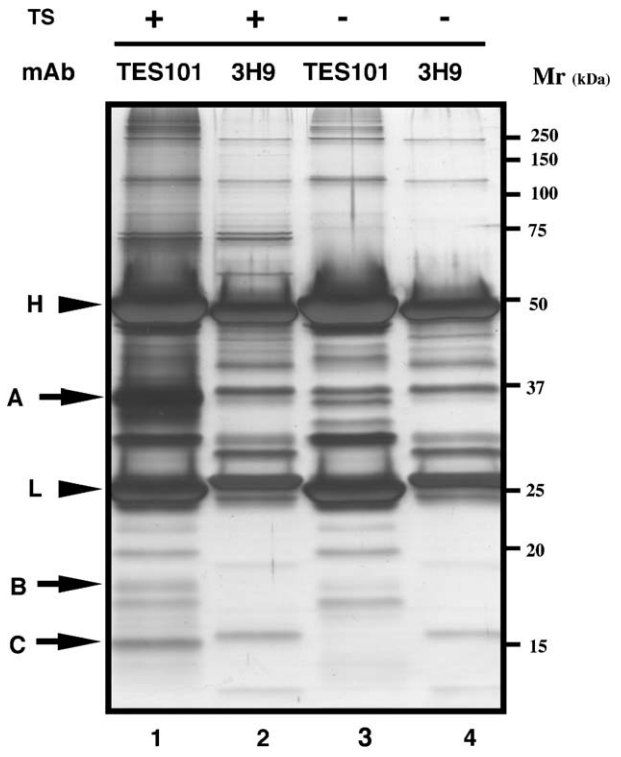

Fig. 1. SDS–PAGE of proteins in mouse testicular Triton® X-100-soluble fraction, co-immunoprecipitated with anti-TEX101 mAb (TES101) visualized by silver staining. The immunoprecipitated proteins from testicular Triton® X-100-soluble fraction (TS) with either TES101 (lane 1) or 3H9 (isotype-match control mAb) (lane 2) were separated by 10% SDS–PAGE under reducing conditions and stained with silver. Control experiments were conducted under the same conditions except for the absence of testicular Triton® X-100-soluble fraction (lanes 3 and 4). Arrows indicate the bands of 36 kDa (A), 18 kDa (B), and 14 kDa (C), co-immunoprecipitated with TES101 mAb from TS. Heavy (H) and light (L) chains of Abs used are showed by arrowheads. M_r, molecular mass.

contained TEX101 (NCBI RefSeq Accession No. NP_064365), with a six-peptide match. A second protein was identified in the same band; however, this protein (annexin 2; NP_031611) was a seven-peptide match (Table 1). Further analysis identified two other bands with apparent molecular masses of 18 and 14 kDa (Fig. 1, 'B' and 'C', lane 1) as ly6k (NP_083903; five-peptide match) and as cellubrevin (NP_033524; two-peptide match), respectively (Table 1). The estimated molecular weights of annexin 2, ly6k, and cellubrevin calculated from their primary amino acid sequence, were similar to those obtained experimentally by reducing SDS–PAGE (Table 1), supporting these identification. In contrast, the apparent molecular mass of TEX101, as determined by reducing SDS–PAGE (~36 kDa), did not correlate with the calculated molecular weight (26,980) of the molecule, due to glycosylation [24].

Confirmation of cellubrevin as a TEX101-associated protein

To confirm the presence of a physical interaction between the proteins identified by LC–MS/MS analysis and TEX101, we performed Western blot analyses on the immunoprecipitated proteins separated by non-reducing SDS–PAGE. As expected, a TES101-immunoreactive band was observed at an apparent molecular mass of 38 kDa (under non-reducing conditions) (Fig. 2A, lane 1). When antibodies specific for cellubrevin or annexin 2 were used as probes, immunoreactive bands were observed at positions corresponding to the expected molecular masses of cellubrevin and annexin 2, respectively (Fig. 2B and C).

As a bi-directional approach, we also examined whether the testicular immunoprecipitant obtained with anti-cellubrevin Ab contained TEX101 and annexin 2. Western blotting with specific Abs to TEX101 and annexin 2 detected specific bands of appropriate mobilities for TEX101 and annexin 2, respectively, in the anti-cellubrevin immunoprecipitant (Fig. 3B and C). When we attempted to perform a parallel experiment examining whether the anti-annexin 2 immunoprecipitant contained TEX101 or cellubrevin, the anti-annexin 2 mAb (purchased from BD Biosciences) did not immunoprecipitate annexin 2 from the testicular fraction (data not shown). In addition, a preliminary immunohistochemical study using the anti-annexin 2 mAb indicated that annexin 2 is localized on the basement membrane, but not in cells within the seminiferous tubules (data not shown). Therefore, annexin 2 appears unlikely to be physically associated with TEX101 or cellubrevin within the testis. As for ly6k protein, we are currently raising mAbs against ly6k to use in biochemical and immunohistochemical studies of its association with TEX101.

Distribution of TEX101and cellubrevin within the testis

The results from our LC–MS/MS analysis and biochemical characterizations suggested that cellubrevin is associated with TEX101 protein. To confirm that this association is physiologically relevant, we examined the localization of cellubrevin and TEX101 within the sexually mature testis using confocal laser immunofluorescence microscopy. TEX101 expression was primarily confined to spermatocytes, spermatids, and spermatozoa (Fig. 4A) as previously reported [20,21]. Cellubrevin, on the other hand, was abundant on haploid germ cells, such as spermatocytes and early-stage spermatids, and was present in relatively small amounts in late-stage spermatids, spermatozoa, spermatogonia, and interstitial cells (Fig. 4B). Examination of the merged TEX101 and cellubrevin fluorescence images demonstrates that an association between the two proteins primarily occurs in spermatocytes and early-stage spermatids (Fig. 4C).

Sub-localization of TEX101 and cellubrevin in spermatogenic cells

Results from confocal laser immunofluorescence microscopy indicated that spermatocytes and round spermatids abundantly express both TEX101 and cellubrevin (Fig. 4). To determine the sites within these germ cells where cellubrevin is associated with TEX101, the subcellular distributions of these molecules were examined by

Table 1
Summary of LC–MS/MS proteomic analysis for the proteins co-immunoprecipitated with TES101 mAb

Band	[a]Exp. M_r	Protein	NCBI RefSeq Accession Number	[b]Cal. M_w	Coverage (%)	[c]Protein score	Peptide identified
A	36 kDa	TEX101	NP_064365	26,980	26	290	TVVLASK DSLASVWR LEFSGGGMDATVQVK GCTTTIGCR LMAMIDSVGPMTVK ETCSYQSFLQPR
		Annexin 2	NP_031611	38,652	24	292	STVHEILCK GVDEVTIVNILTNR ELPSALK SALSGHLETVILGLLK TPAQYDASELK GLGTDEDSLIEIICSR TNQELQEINR
B	18 kDa	Ly6k	NP_083903	17,123	31	164	KFCLLAVTR FFYVSK RCPTPVVSPPSTNPPSEPK EFLIEK PMPFLFYK
C	14 kDa	Cellubrevin	NP_033524	11,473	33	65	LQQTQNQVDEVVDIMR ADALQAGASQFETSAAK

[a] Exp. M_r, experimental molecular mass on SDS–PAGE under reducing conditions.
[b] Cal. M_w, calculated molecular weight from primary protein sequence without posttranslational modifications.
[c] Protein score, the value was calculated by Mascot search.

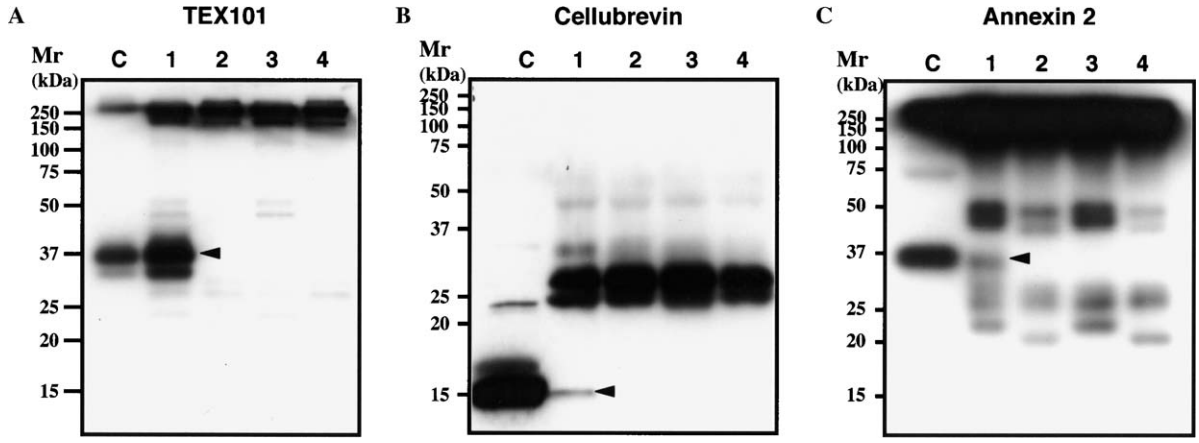

Fig. 2. Western blot analysis of proteins in mouse testicular Triton® X-100-soluble fraction co-immunoprecipitated with TES101 mAb. Experimental conditions for immunoprecipitation with TES101 or 3H9 were identical for the experiments shown in Fig. 1 (lanes 1–4). After immunoprecipitation, the proteins were separated by SDS–PAGE under non-reducing (A,C) or reducing (B) conditions and then transferred onto a PVDF membrane. Immunoreactivity using anti-TEX101(A), cellubrevin (B), or annexin 2 (C) Abs was monitored by ECL detection system as described in Materials and methods. Aliquot of testicular Triton® X-100-soluble fraction was used as a positive control for Western blotting (lane C). Specific immunoreactivity observed in the lanes 1 in (A, B, and C) are indicated by arrowheads.

UHR-IFM using ultrathin cryosections (⩽100-nm thick in the *z*-dimension). These cryosections are thin enough to render negligible the coincidence (overlap) of overlying organelles [32]. In comparison, the *z*-resolution achieved in confocal microscopy of biological samples is typically 500 nm or greater [33]. In UHR-IFM, the high sampling efficiency of immunofluorescence allows examination of thousands of subcellular structures at ultrahigh resolution.

The extraordinary thinness of the cryosections allowed accurate analysis of the association between TEX101 and cellubrevin. Consistent with our confocal microscopic observations (Fig. 4), strong anti-cellubrevin immunostaining was present in spermatocytes and round spermatids (Fig. 5A2–C2), whereas immunostaining of elongating spermatids, spermatogonia, and Sertoli cells was negligible (Fig. 5A2 and B2). Precise subcellular observations demonstrated that cellubrevin is present primarily in the cytoplasmic region in the spermatocytes and spermatids with punctate staining (Fig. 6). Cellubrevin-positive immunostaining was frequently observed

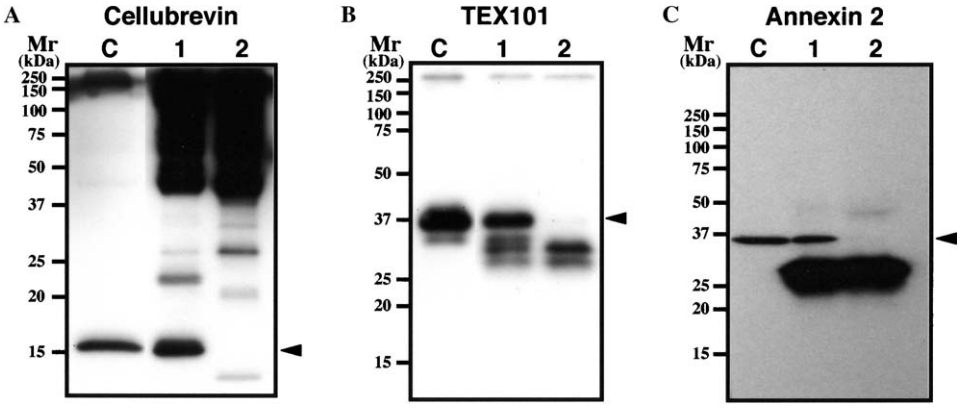

Fig. 3. Western blot analysis of proteins in mouse testicular Triton® X-100-soluble fraction co-immunoprecipitated with anti-cellubrevin Ab. The immunoprecipitated proteins from testicular Triton® X-100-soluble fraction with either anti-cellubrevin Ab (lane 1) or normal rabbit Ig (lane 2) were separated by SDS–PAGE under non-reducing (A,B), or reducing (C) conditions. Western blot was performed using the primary Abs against cellubrevin (A), TEX101 (B), and annexin 2 (C). The testicular Triton® X-100-soluble fraction was used as a positive control (lane C). The immunoreactive bands are indicated by arrowheads, respectively.

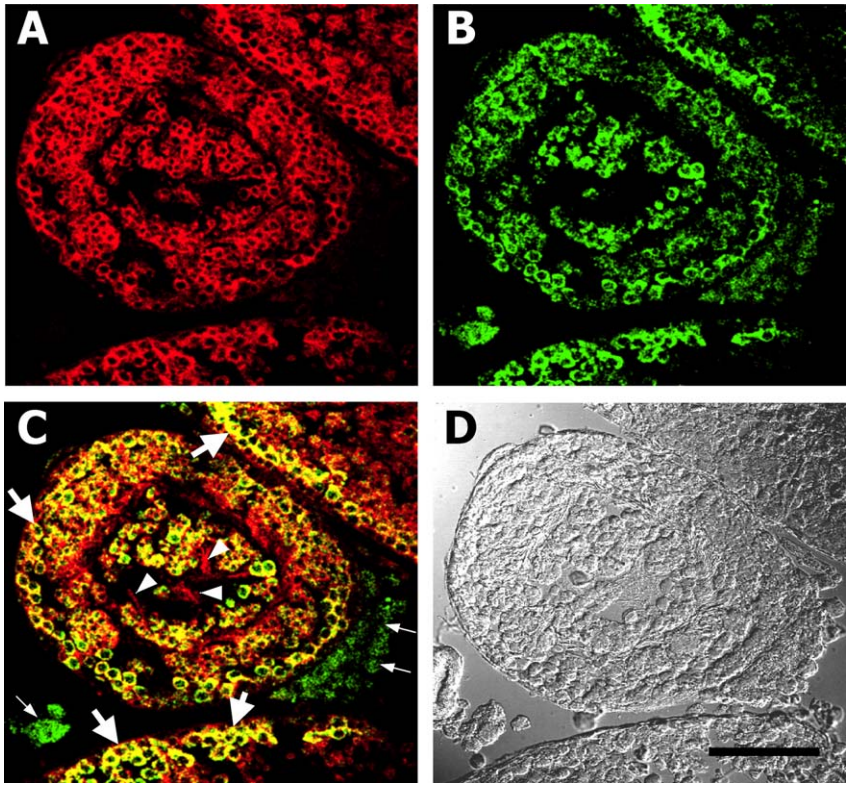

Fig. 4. Immunolocalization of TEX101 and cellubrevin within sexually mature mouse testis observed with confocal lazer microscopy. The fluorescent images of TEX101 (red) (A), cellubrevin (green) (B), their overlay (C), and differential interference contrast image (D). The immunoreactivities overlapped with both TEX101 and cellubrevin are observed in spermatocytes and round spermatids (large arrows). Arrowheads indicate elongating spermatids and testicular spermatozoa reactive with TES101, but not anti-cellubrevin Ab. Interstitial cells with only positive staining of cellubrevin are shown by small arrows. Bar, 50 μm.

both on and immediately beneath the cell surface membrane (Fig. 6).

As previously demonstrated [20,21], intense immunostaining with TES101 mAb was observed throughout the plasma membranes of spermatocytes and spermatids, but not spermatogonia or Sertoli cells (Fig. 5A1–C1). This experiment also produced the novel observation that TEX101 exhibited a spotted distribution in the spermatocyte and spermatid cytoplasms, where most of this intracellular staining overlapped with cellubrevin immunostaining (Fig. 6), although some intracellular cellubrevin molecules did not appear to be associated with TEX101. Both molecules also co-localized on the cell surfaces (Fig. 6). Notably, in most cases, cellubrevin was located adjacent to, but not

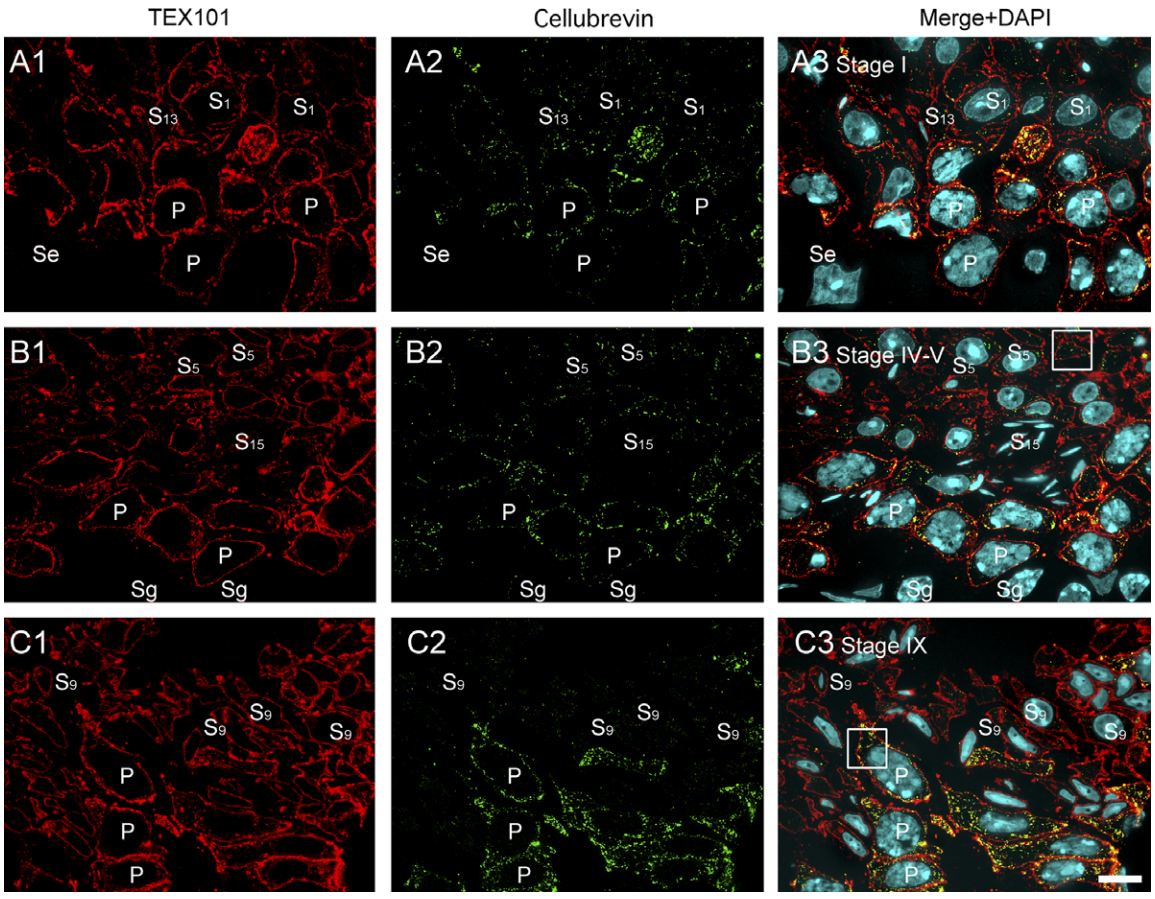

Fig. 5. Subcellular localization of TEX101 and cellubrevin within seminiferous tubules of mouse testis examined by UHR-IFM: lower magnification images. Mouse testicular ultrathin cryosections double-stained for TEX101 (red) and cellubrevin (green) with nuclear counterstaining of DAPI (blue) were observed with immunofluorescent microscopy. The immunofluorescent images of TEX101 (1), cellubrevin (2), their overlay with DAPI (3) in the stage I (A), IV–V (B), and IX (C) of the seminiferous tubules. Pachytene-type spermatocytes (P), spermatids (S), Sertoli cells (Se), and spermatogonia (Sg) were evident. Bar, 10 μm.

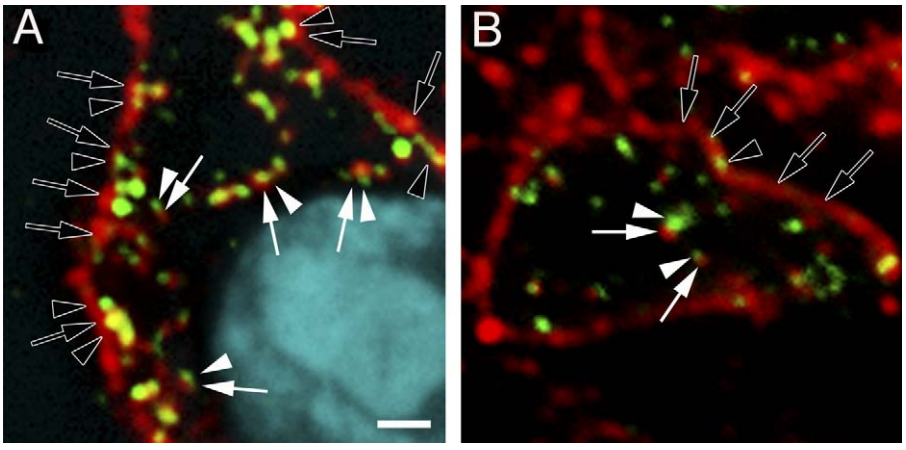

Fig. 6. Subcellular localization of TEX101 and cellubrevin in the spermatocyte and spermatid: higher magnification images. Pachytene-type spermatocyte (A) and the step 5 of spermatid (B) surrounded by white squares in Fig. 5B3 and C3, respectively. Color definitions are identical as shown in Fig. 5. TEX101 is primarily localized on throughout the cell surface (black arrows) with minor intracellular staining (white arrows). The localization of cellubrevin is observed on both the plasma membrane (black arrowheads) and intracellular structures (white arrowheads). Cellubrevin is juxtaposed with TEX101 both just below the plasma membrane and in the cytoplasmic regions. Bar, 1 μm.

fully overlapped with, TEX101. Intracellular cellubrevin appeared to be juxtaposed with intracellular TEX101, and membrane-associated cellubrevin appeared to be docked near TEX101-positive plasma membranes on the cytoplasmic side (Fig. 6). An association between the two molecules was never observed on the cell surface (Fig. 6).

This series of immunohistochemical findings leads us to conclude that physical associations between cellubrevin and TEX101 occur primarily in the cytoplasmic compartment and immediately beneath the cell surface in spermatocytes and early-stage spermatids.

Discussion

Generally, protein molecules carry out their physiological actions via interactions with other proteins [25]. Elucidation of the functional and physical networks that exist among proteins is of fundamental importance in understanding their functions and their regulatory mechanisms [25,34]. The emerging field of proteomics has provided powerful tools for functional studies of protein–protein interactions[34,35]; such developments have been largely due to advances in MS sample preparation, analytical sensitivity, and instrumental software, and to the expansion of protein databases [36].

The experimental results described herein, obtained from immunoprecipitation-LC–MS/MS proteomics and immunofluorescence studies, including UHR-IFM analysis, clearly demonstrate that cellubrevin (a member of the family of soluble *N*-ethylmaleimide-sensitive factor attachment protein receptors (SNAREs)) associates with TEX101, a cell-surface marker unique to male and female germ cells [20–22,24,37]. To date, many lines of evidence have shown that SNAREs play a central role in the control of membrane trafficking and fusion [38]. On the basis of their structural similarities, mammalian SNAREs have been further subcategorized as syntaxins, vesicle-associated membrane proteins (VAMPs) or 25-kDa synaptosomal-associated proteins (SNAP-25s) [39,40]. SNAREs commonly contain membrane-tethering structures and cytoplasmic, α-helical coiled-coil domains [41,42] that evolved, presumably, from a common ancestor with a hydrophobic heptad register, interrupted by a conserved polar residue [43] at the ionic "zero" layer [44]. Depending on the nature of this polar residue, SNAREs have been reclassified as either glutamine (Q)- or arginine (R)-SNAREs [40].

In the exo/endocytotic processes, vesicle fusion is mediated by heterotetrameric SNARE complexes consisting of three Q-SNAREs (syntaxin/SNAP-25) and one R-SNARE (VAMP); These complexes are stabilized by tight bundling of the SNARE coiled-coil domains [40]. In most cases, the R-SNARE is localized on the vesicles, and the Q-SNAREs are present on the target organelle [40,41]. Cellubrevin (VAMP3) is a member of the VAMP subfamily and is primarily localized in the vesicle membrane, where it is anchored by its C-terminal, transmembrane domain [45,46]. Cellubrevin-dependent trafficking is involved in the recycling of plasma membrane receptors, such as the transferrin receptor [47], or T-cell receptor to an immunological synapse [48]. It also participates in the early endosomal pathways involving apical transport of H^+-ATPase [49], focal contacts in phagocytosis [50], cell adhesion, and cell migration [51]. Studies published in the past decade have gradually revealed that cellubrevin is able to localize to the plasma membrane, where it participates in exocytotic vesicle fusion, although it is believed to generally reside in endosomal vesicles.

Using immunofluorescence microscopic analysis, we have demonstrated that cellubrevin is abundantly expressed in certain germ cells, such as spermatocytes and early-stage spermatids (Figs. 4 and 5), while pachytene spermatocytes express large amounts of intracellular TEX101 (Figs. 5 and 6). Recent in situ hybridization studies have demonstrated that *TEX101* mRNA is expressed in spermatocytes and step 1–9 spermatids, but not in spermatogonia [22], indicating that de novo synthesis of TEX101 closely correlates with abundant cellubrevin expression in male germ cells during spermatogenesis. Results of UHR-IFM studies using ultrathin cryosections revealed a punctate distribution of cellubrevin on the plasma membrane and in the cytoplasmic region of meiotic cells, where some cellubrevin co-localized with TEX101 (Figs. 5 and 6). A notable finding was also provided that cellubrevin is attached with TEX101 immediately beneath the cell surface but, in many cases, it does not completely overlap on the cell membrane (Fig. 6). Taken together, these results strongly suggest that cellubrevin plays an important role in membrane trafficking of *de novo* TEX101 to the cell surface, and that the cellubrevin-dependent membrane trafficking system may be required for correct spatiotemporal expression of TEX101 during spermatogenesis.

Immunoprecipitation of the testicular Triton® X-100-soluble fraction with TES101 mAb led us to identify annexin 2 (Table 1 and Fig. 2) in the same ~36 kDa SDS gel band as TEX101 (Fig. 1, 'A', lane 1). This molecule was also recovered from the testicular Triton® X-100-soluble fraction by immunoprecipitation with anti-cellubrevin Ab (Fig. 3). Although these results raise the possibility that annexin 2 forms a multimeric complex with TEX101 and cellubrevin, an immunohistochemical study using anti-annexin 2 mAb did not support this possibility. Immunofluorescence using anti-annexin 2 mAb showed that annexin 2 is localized on the basement membrane of the seminiferous tubules, not in germ cells (data not shown). Therefore, annexin 2 is highly unlikely to be associated with TEX101 within testis. At present, however, the absence of annexin 2 in other areas of the testis cannot be confirmed completely because its mAb epitope might be disturbed by protein–protein interactions, perhaps within the seminiferous tubules. The failure of reciprocal IP with anti-annexin 2 antibody (data not shown) may also be due to epitope masking. Further biochemical and immunohistochemical studies will be necessary to resolve this issue.

We also identified ly6k as a candidate TEX101-associated testicular protein (Fig. 1 and Table 1). Ly6k is a typical ly6 family member with conserved molecular features [52]. Like other ly6 antigens, this small molecule has 10 conserved cysteine residues and harbors the sequence that theoretically defines the GPI-anchoring site at its C-terminus

[52]. Like ly6k, TEX101 is a GPI-anchored protein lacking an intracellular domain. [24]. Several lines of evidence have suggested that ly6 family members are involved in cell signaling and activation such as activation and differentiation of T cells [53–55]. Taken together, a complex including these molecules may constitute a functional membrane unit for germ-cell differentiation. We speculate that these GPI-anchored proteins associate with a transmembrane protein that transduces the extracellular signal to intracellular molecules.

To confirm the physiological association between these molecules and uncover the whole constitution of TEX101/ly6k membrane complex, we are currently undertaking to produce mAbs applicable to a variety of experimental studies. To confirm the physiological association between these molecules and to identify the entire complement of proteins in the TEX101/ly6k membrane complex, we are currently raising mAbs applicable to a variety of experimental approaches.

In summary, we have confirmed that a physiological association between cellubrevin and TEX101 exists in spermatocytes and early-stage spermatids. We propose that the cellubrevin-dependent membrane trafficking system is necessary for the precise spatiotemporal expression of TEX101 in male germ cells. The molecular function and germ cell-specific expression kinetics results of this study provide us with some clues that hint at the physiological role of TEX101 in the fundamental molecular mechanism of spermatogenesis. The role of TEX101 in gametogenesis should be further clarified by studies we are currently conducting that examine the association of TEX101 with ly6k.

Acknowledgments

The authors are gratefully acknowledged for the staff of the Animal facility, Juntendo University for their technical supports. This work was supported in part by Grants-in-Aid for ''High-Tech Research Center'' Project for Private Universities: matching fund subsidy and General Scientific Research No. 16591635 and 18591813 from the Ministry of Education, Culture, Sports, Science and Technology, Japan.

References

[1] Y. Clermont, Kinetics of spermatogenesis in mammals: seminiferous epithelium cycle and spermatogonial renewal, Physiol. Rev. 52 (1972) 198–236.
[2] R.A. Hess, Quantitative and qualitative characteristics of the stages and transitions in the cycle of the rat seminiferous epithelium: light microscopic observations of perfusion-fixed and plastic-embedded testes, Biol. Reprod. 43 (1990) 525–542.
[3] N. Ravidranath, L. Dettin, M. Dym, Mammalian testis: structure and function, in: D.R.P. Tulsiani (Ed.), Introduction to Mammalian Reproduction, Kluwer Academic Publishers, Boston, 2003, pp. 1–19.
[4] M. Fujisawa, Cell-to-cell cross talk in the testis, Urol. Res. 29 (2001) 144–151.
[5] M.K. Siu, C.Y. Cheng, Dynamic cross-talk between cells and the extracellular matrix in the testis, Bioessays 26 (2004) 978–992.
[6] R.W. Holdcraft, R.E. Braun, Hormonal regulation of spermatogenesis, Int. J. Androl. 27 (2004) 335–342.
[7] S. Kimmins, N. Kotaja, I. Davidson, P. Sassone-Corsi, Testis-specific transcription mechanisms promoting male germ-cell differentiation, Reproduction 128 (2004) 5–12.
[8] N.B. Hecht, Molecular mechanisms of male germ cell differentiation, Bioessays 20 (1998) 555–561.
[9] H. Tanaka, Y. Yoshimura, Y. Nishina, M. Nozaki, H. Nojima, Y. Nishimune, Isolation and characterization of cDNA clones specifically expressed in testicular germ cells, FEBS Lett. 355 (1994) 4–10.
[10] T. Fujii, K. Tamura, K. Masai, H. Tanaka, Y. Nishimune, H. Nojima, Use of stepwise subtraction to comprehensively isolate mouse genes whose transcription is up-regulated during spermiogenesis, EMBO Rep. 3 (2002) 367–372.
[11] K. Tanaka, H. Tamura, H. Tanaka, M. Katoh, Y. Futamata, N. Seki, Y. Nishimune, T. Hara, Spermatogonia-dependent expression of testicular genes in mice, Dev. Biol. 246 (2002) 466–479.
[12] D.G. de Rooij, P. de Boer, Specific arrests of spermatogenesis in genetically modified and mutant mice, Cytogenet. Genome Res. 103 (2003) 267–276.
[13] B.H. Schrans-Stassen, P.T. Saunders, H.J. Cooke, D.G. de Rooij, Nature of the spermatogenic arrest in Dazl −/− mice, Biol. Reprod. 65 (2001) 771–776.
[14] D. Zhang, T.L. Penttila, P.L. Morris, M. Teichmann, R.G. Roeder, Spermiogenesis deficiency in mice lacking the Trf2 gene, Science 292 (2001) 1153–1155.
[15] I. Mendoza-Lujambio, P. Burfeind, C. Dixkens, A. Meinhardt, S. Hoyer-Fender, W. Engel, J. Neesen, The Hook1 gene is non-functional in the abnormal spermatozoon head shape (azh) mutant mouse, Hum. Mol. Genet. 11 (2002) 1647–1658.
[16] S.M. Lipkin, P.B. Moens, V. Wang, M. Lenzi, D. Shanmugarajah, A. Gilgeous, J. Thomas, J. Cheng, J.W. Touchman, E.D. Green, P. Schwartzberg, F.S. Collins, P.E. Cohen, Meiotic arrest and aneuploidy in MLH3-deficient mice, Nat. Genet. 31 (2002) 385–390.
[17] G. Hamer, H.B. Kal, C.H. Westphal, T. Ashley, D.G. de Rooij, Ataxia telangiectasia mutated expression and activation in the testis, Biol. Reprod. 70 (2004) 1206–1212.
[18] H. Tanaka, N. Iguchi, C. Egydio de Carvalho, Y. Tadokoro, K. Yomogida, Y. Nishimune, Novel actin-like proteins T-ACTIN 1 and T-ACTIN 2 are differentially expressed in the cytoplasm and nucleus of mouse haploid germ cells, Biol. Reprod. 69 (2003) 475–482.
[19] H. Ohta, K. Yomogida, K. Dohmae, Y. Nishimune, Regulation of proliferation and differentiation in spermatogonial stem cells: the role of c-kit and its ligand SCF, Development 127 (2000) 2125–2131.
[20] A. Kurita, T. Takizawa, T. Takayama, K. Totsukawa, S. Matsubara, H. Shibahara, M.-C. Orgebin-Crist, F. Sendo, Y. Shinkai, Y. Araki, Identification, cloning, and initial characterization of a novel mouse testicular germ cell-specific antigen, Biol. Reprod. 64 (2001) 935–945.
[21] T. Takayama, T. Mishima, M. Mori, H. Jin, H. Tsukamoto, K. Takahashi, T. Takizawa, K. Kinoshita, M. Suzuki, I. Sato, S. Matsubara, Y. Araki, T. Takizawa, Sexually dimorphic expression of the novel germ cell antigen TEX101 during mouse gonad development, Biol. Reprod. 72 (2005) 1315–1323.
[22] T. Takayama, T. Mishima, M. Mori, T. Ishikawa, T. Takizawa, T. Goto, M. Suzuki, Y. Araki, S. Matsubara, T. Takizawa, Mouse TEX101 is shed from the cell surface of sperm in the caput epididymidis, Zygote 13 (2005) 325–333.
[23] S. Udenfriend, K. Kodukula, How glycosylphosphatidylinositol-anchored membrane proteins are made, Annu. Rev. Biochem. 64 (1995) 563–591.
[24] H. Jin, H. Yoshitake, H. Tsukamoto, M. Takahashi, M. Mori, T. Takizawa, K. Takamori, H. Ogawa, K. Kinoshita, Y. Araki, Molecular characterisation of a germ cell-specific antigen, TEX101, from mouse testis, Zygote (2006) in press.
[25] T. Pawson, P. Nash, Assembly of cell regulatory systems through protein interaction domains, Science 300 (2003) 445–452.
[26] K. Ohtake, H. Takei, T. Watanabe, Y. Sato, T. Yamashita, K. Sudo, M. Kuroki, J. Chihara, F. Sendo, A monoclonal antibody modulates

neutrophil adherence while enhancing cell motility, Microbiol. Immunol. 41 (1997) 67–72.
[27] U.K. Laemmli, Cleavage of structural proteins during the assembly of the head of bacteriophage T4, Nature 227 (1970) 680–685.
[28] A. Shevchenko, M. Wilm, O. Vorm, M. Mann, Mass spectrometric sequencing of proteins silver-stained polyacrylamide gels, Anal. Chem. 68 (1996) 850–858.
[29] Y. Araki, M.E. Vierula, T.L. Rankin, D.R. Tulsiani, M.-C. Orgebin-Crist, Isolation and characterization of a 25-kilodalton protein from mouse testis: sequence homology with a phospholipid-binding protein, Biol. Reprod. 47 (1992) 832–843.
[30] Y. Takeda, J. Fu, K. Suzuki, D. Sendo, T. Nitto, F. Sendo, Y. Araki, The expression of GPI-80, a number of the aminohydrolase family, requires neutrophil differentiation with dimethylsulfoxide in HL-60 cells, Exp. Cell Res. 286 (2003) 199–208.
[31] T. Takizawa, J.M. Robinson, Ultrathin cryosections: an important tool for immunofluorescence and correlative microscopy, J. Histochem. Cytochem. 51 (2003) 707–714.
[32] T. Takizawa, C.L. Anderson, J.M. Robinson, A novel FcγR-defined,IgG-containing IgG-containing organelle in placental endothelium, J. Immunol. 175 (2005) 2331–2339.
[33] L. Majlof, P.O. Forsgren, Confocal microscopy: important considerations for accurate imaging, Methods Cell Biol. 38 (1993) 79–95.
[34] T. Natsume, Y. Yamauchi, H. Nakayama, T. Shinkawa, M. Yanagida, N. Takahashi, T. Isobe, A direct nanoflow liquid chromatography-tandem mass spectrometry system for interaction proteomics, Anal. Chem. 74 (2002) 4725–4733.
[35] H. Zhu, M. Bilgin, M. Snyder, Proteomics, Annu. Rev. Biochem. 72 (2003) 783–812.
[36] M. Mann, R.C. Hendrickson, A. Pandey, Analysis of proteins and proteomes by mass spectrometry, Annu. Rev. Biochem. 70 (2001) 437–473.
[37] H. Tsukamoto, T. Takizawa, K. Takamori, H. Ogawa, Y. Araki, Genomic organization and structure of the 5′-flanking region of the TEX101 gene: Alternative promoter usage and splicing generate transcript variants with distinct 5′-untranslated region, Mol. Reprod. Dev. (2006) in press.
[38] Y.A. Chen, R.H. Scheller, SNARE-mediated membrane fusion, Nat. Rev. Mol. Cell Biol. 2 (2001) 98–106.
[39] V. Rossi, R. Picco, M. Vacca, M. D'Esposito, M. D'Urso, T. Galli, F. Filippini, VAMP subfamilies identified by specific R-SNARE motifs, Biol. Cell 96 (2004) 251–256.
[40] D. Fasshauer, R.B. Sutton, A.T. Brunger, R. Jahn, Conserved structural features of the synaptic fusion complex: SNARE proteins reclassified as Q- and R-SNAREs, Proc. Natl. Acad. Sci. USA 95 (1998) 15781–15786.
[41] J.C. Hay, SNARE complex structure and function, Exp. Cell Res. 271 (2001) 10–21.
[42] D. Ungar, F.M. Hughson, SNARE protein structure and function, Annu. Rev. Cell Dev. Biol. 19 (2003) 493–517.
[43] T. Weimbs, K. Mostov, S.H. Low, K. Hofmann, A model for structural similarity between different SNARE complexes based on sequence relationships, Trends Cell Biol. 8 (1998) 260–262.
[44] R.B. Sutton, D. Fasshauer, R. Jahn, A.T. Brunger, Crystal structure of a SNARE complex involved in synaptic exocytosis at 2.4Å resolution, Nature 395 (1998) 347–353.
[45] H.T. McMahon, Y.A. Ushkaryov, L. Edelmann, E. Link, T. Binz, H. Niemann, R. Jahn, T.C. Sudhof, Cellubrevin is a ubiquitous tetanus-toxin substrate homologous to a putative synaptic vesicle fusion protein, Nature 364 (1993) 346–349.
[46] V. Proux-Gillardeaux, R. Rudge, T. Galli, The tetanus neurotoxin-sensitive and insensitive routes to and from the plasma membrane: fast and slow pathways? Traffic 6 (2005) 366–373.
[47] T. Galli, T. Chilcote, O. Mundigl, T. Binz, H. Niemann, P. De Camilli, Tetanus toxin-mediated cleavage of cellubrevin impairs exocytosis of transferrin receptor-containing vesicles in CHO cells, J. Cell Biol. 125 (1994) 1015–1024.
[48] V. Das, B. Nal, A. Dujeancourt, M.I. Thoulouze, T. Galli, P. Roux, A. Dautry-Varsat, A. Alcover, Activation-induced polarized recycling targets T cell antigen receptors to the immunological synapse; involvement of SNARE complexes, Immunity 20 (2004) 577–588.
[49] S. Breton, N.N. Nsumu, T. Galli, I. Sabolic, P.J. Smith, D. Brown, Tetanus toxin-mediated cleavage of cellubrevin inhibits proton secretion in the male reproductive tract, Am. J. Physiol. Renal Physiol. 278 (2000) F717–F725.
[50] L. Bajno, X.R. Peng, A.D. Schreiber, H.P. Moore, W.S. Trimble, S. Grinstein, Focal exocytosis of VAMP3-containing vesicles at sites of phagosome formation, J. Cell Biol. 149 (2000) 697–706.
[51] V. Proux-Gillardeaux, J. Gavard, T. Irinopoulou, R.M. Mege, T. Galli, Tetanus neurotoxin-mediated cleavage of cellubrevin impairs epithelial cell migration and integrin-dependent cell adhesion, Proc. Natl. Acad. Sci. USA 102 (2005) 6362–6367.
[52] A.G. de Nooij-van Dalen, G.A. van Dongen, S.J. Smeets, E.J. Nieuwenhuis, M. Stigter-van Walsum, G.B. Snow, R.H. Brakenhoff, Characterization of the human Ly-6 antigens, the newly annotated member Ly-6k included, as molecular markers for head-and-neck squamous cell carcinoma, Int. J. Cancer 103 (2003) 768–774.
[53] T.P. Gumley, I.F. McKenzie, M.S. Sandrin, Tissue expression, structure and function of the murine Ly-6 family of molecules, Immunol. Cell Biol. 73 (1995) 277–296.
[54] A. Bamezai, Mouse Ly-6 proteins and their extended family: markers of cell differentiation and regulators of cell signaling, Arch. Immunol. Ther. Exp. 52 (2004) 255–266.
[55] A. Bamezai, D. Palliser, A. Berezovskaya, J. McGrew, K. Higgins, E. Lacy, K.L. Rock, Regulated expression of Ly-6A.2 is important for T cell development, J. Immunol. 154 (1995) 4233–4239.